JOURNAL OF THEORETICAL
AND APPLIED MECHANICS
51, 4, pp. 1003-1012, Warsaw 2013

STRESS CONCENTRATION ON THE CONTOUR OF A PLATE OPENING: ANALYTICAL, NUMERICAL AND EXPERIMENTAL APPROACH

Nikola Momcilovic, Milorad Motok, Tasko Maneski
University of Belgrade, Faculty of Mechanical Engineering, Belgrade, Serbia
e-mail: nmomcilovic@mas.bg.ac.rs; mmotok@mas.bg.ac.rs; tmaneski@mas.bg.ac.rs

The objective of the paper is to analyze the stress concentration factor (SCF) in the corner of a rectangular plate opening with small radii of curvature and various methods for its derivation. Besides the finite element method, as the most used approach today, there are some analytical and experimental procedures that can obtain stress concentration results in such spots. An analytical approach can deliver prediction of the SCF around the corner but cannot illustrate the stress field opposite to the finite element method. On the other hand, finite element analysis needs much computation time to deal with very sensitive and fine mesh generation around concentration zones. Experimental devices, such as strain gauges are not able to perform measurements on areas where high gradient of stress occurs due to their lack of sensitiveness and larger dimensions compared to the measured part of a structure. The paper presents Digital Image Correlation (DIC) technique that obtains not only stress concentration, where other devices fail, but also provides full displacement, strain and stress field's even where a high gradient of stress exists. These three methods are discussed, compared and illustrated on the model of a plate with rectangular opening subjected to tension.

Key words: stress concentration factor (SCF), digital image correlation (DIC), plate opening, small radius of curvature

1. Introduction

Plate openings with some kind of rounded corners are inevitable in structures, whether made by a manufacturing process or for the reason of decreasing stress concentration. Stress concentration in zones with a small radius of curvature on a contour of the plate opening seems a very significant issue in strength problems (Kopecki, 2011; Laughalam *et al.*, 2011; Rezaeepazhand and Jafari, 2010; Motok, 1997), especially in ship structures such as deck openings, scallops, aircraft fuselages or tail planes. The presence of an opening makes even a simple structure model complicated to analyze regardless of the method being used. In order to deal with this problem, three possible approaches appear: analytical, numerical and experimental. Every one of them has advantages and issues, although their ongoing techniques are constantly being updated and modernized.

Stress concentration in a plate under tension and weakened by a hole was recognized long time ago, and basic analytical solutions were presented by Muskhelishvilli (1953) and further utilized by Savin (1961). More recently, some other solutions were derived (Laughalam *et al.*, 2011; Motok, 1997). The main problem of the analytical approach seems to be the difficulty to analytically express the contour of a rectangular opening with a small and variable corner radius.

As far as numerical methods are concerned, a very fine mesh is needed in order to obtain realistic stress results around the critical zone. Although nowadays modern finite element based software has possibility to analyze models with large degrees of freedom that significantly increases the computation time.

Experimental methods remain the most confident methods to measure real behavior of structures with openings (Maneski and Milosevic-Mitic, 2010; Guo *et al.*, 2009; Toubal *et al.*, 2005). Nevertheless, it is very hard (almost impossible) to "catch" stress concentration by means of classical measuring devices (strain gauges, inductive sensors) where a large gradient exists. Fortunately, some "state of the art" experimental nondestructive methods, like Digital Image Correlation Method – DIC (Sutton, 2008; Hild and Roux, 2006; Lecompte *et al.*, 2006), holographic interferometry, speckle interferometry, Moiré interferometry are available today. The holographic and speckle interferometry are used for displacements and shape measurement of optically rough surfaces at sensitivity of the order of the wavelength of light. In the holographic interferometry (Kreis, 2005; Jones and Wykes, 1989), three-dimensional information about the surface of an object is recorded by a hologram. Changed geometry of the surface, upon being subjected to load, is compared to the formerly recorded state. Surface changes are observed as a series of interference fringes superimposed on the image of the object in order to obtain displacements. The speckle interferometry (Jones and Wykes, 1989) is based on a random interference pattern observed when coherent laser light is scattered from a rough surface. The information about the object, in Moiré interferometry (Post, 1987), is acquired as interference fringe patterns (or contour maps) of the displacement fields with high sensitivity. Furthermore, trustworthy strain distributions are extracted from these patterns. This method, as oppose to classical inteferometry that is most effective for out of plane displacements, is widely recognized for obtaining in-plane displacements. Digital Image Correlation is discussed in Section 4 regarding the experimental approach being used in the presented measurement.

In this paper, analytical, numerical and experimental techniques that may obtain stress concentration results for the discussed problem properly are presented. The idea is to illustrate and compare those methods on the example of a plate weakened by a rectangular opening with a small corner radius of curvature and subjected to tension.

The analyzed plate (Fig. 1) with overall dimensions of $1000\,\mathrm{mm}\times1000\,\mathrm{mm}\times2\,\mathrm{mm}$ is made of structural steel S235JRG2 with the modulus of elasticity $E = 200000\,\mathrm{N/mm^2}$, Poisson's ratio $\nu = 0.3$ and the yield stress $\sigma_y = 240\,\mathrm{N/mm^2}$. The plate is weakened by a rectangular opening ($300\,\mathrm{mm}\times300\,\mathrm{mm}$) with corner radii of 0.5, 1, 2 and 3 mm. That allowed exploration pf one experimental model to provide results for four different corner radii. The plate is subjected to in-plain tension.

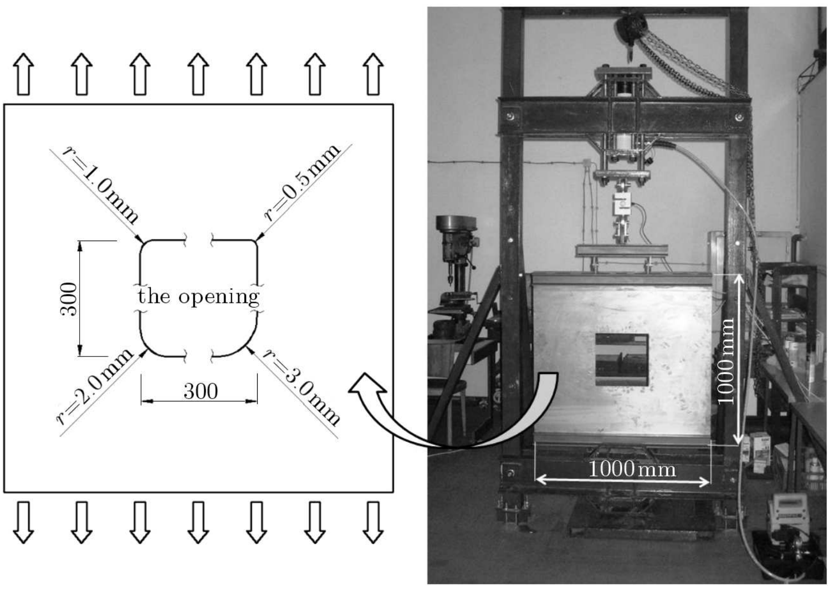

Fig. 1. Analyzed plate

2. Analytical approach

The formula defined by Motok (1997) is chosen as an analytical procedure to obtain SCF results for the analyzed model. The algorithm is derived from Muskhesvili's solution for the problem of an infinite plate subjected to tension and weakened by a hole the contour of which can be defined by means of conformal mapping (Fig. 2). These solutions were practically applicable for

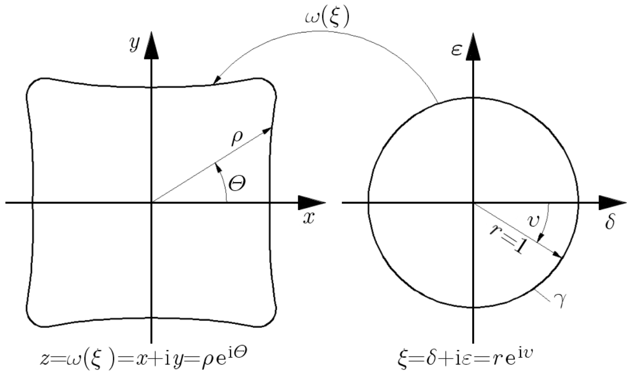

Fig. 2. Mapping of a unit circle into a square

a narrow spectrum of the corner radius of curvature only. The functions of a complex variable $\omega(\xi)$ for mapping a unit circle into a square, rectangular or hexagonal contours can be derived from the Schwarz-Christoffel integral. If complete series (i.e. with an infinite number of terms) resulting from the integral are used, the mapped contours achieve shapes of regular polygons with straight sides and no curvatures in the corners. By decreasing the number of terms used in the mapping, the curvilinear contours can be obtained. The radius of curvature on their sides and in the corners is greater as the number of used terms is smaller. Therefore, using an appropriate number of terms, the contours of an arbitrary small corner can be analyzed. However, since the conformal mapping presumes making use of functions of the complex variable, evaluation of stresses demands using of basic equations of theory of elasticity in a complex form. Derived final formula (2.1) for SCF in the corner of a square opening of an arbitrary small radius of curvature still appears to be easy to use (C_i coefficients in Table 1 are improved versions of the original ones (Motok, 1997)). SCF is taken as the ratio of maximal principal stress in the corner on the contour and the nominal tension load applied to the plate; a/r is the ratio of the overall dimension of the opening ($a = 300\,\mathrm{mm}$) and the corner radius

$$\mathrm{SCF} = \sum_{i=0}^{10} C_i\Big(\frac{a}{r}\Big)^i \tag{2.1}$$

Table 1. C_i coefficients

i	C_i	i	C_i
0	3.1002	6	−1.753E-14
1	0.087697	7	1.4196E-17
2	−5.322E-04	8	−7.158E-21
3	2.4609E-06	9	2.0415E-24
4	−7.304E-09	10	−2.514E-28
5	1.4011E-11		

Expression (2.1) is simple, ready for instant use and applicable for the presented problem. The formula is limited to local strength analyses only, but due to its straightforwardness, it can be especially practicable in quick solving of practical problems.

3. Finite element approach

As a standard method incorporated in modern software engineering tools, the finite element method (FEM) presents a powerful numerical device for obtaining the stress field in a concentration zone of a structure, especially regarding small geometrical discontinuities, such as openings, cutouts, various imperfections (Laughalam *et al.*, 2011; Madani *et al.*, 2010; Kopecki, 2010; Guo *et al.*, 2009; Ukadgaonker and Kakhandki, 2005; Wu and Mu, 2003; Chen, 1993). Still, the need for an extremely fine mesh around corners increases computation time drastically. Modern FEM based software such as one used for the purpose of this analysis – Komips (Maneski, 2005) works with an extremely high number of degrees of freedom and is able to generate a large density mesh around areas of high stress gradient. Yet, the radius of 0.5 or 1 mm, such as in this case, is still a very small dimension (compared to the dimensions of the opening and plate themselves), and it is not easy to produce a mesh that would illustrate the high stress gradient properly. Based on several models of the same plate with different mesh density (Fig. 3), it is concluded that the minimum of eight divisions is needed to describe the radius geometrically and obtain convergence in the stress concentration field. It means that what seems to be a simple model of the plate has to be meshed with a significantly increased number of elements just because of the presence of these four corner areas. The final number of shell elements in the model is 8787.

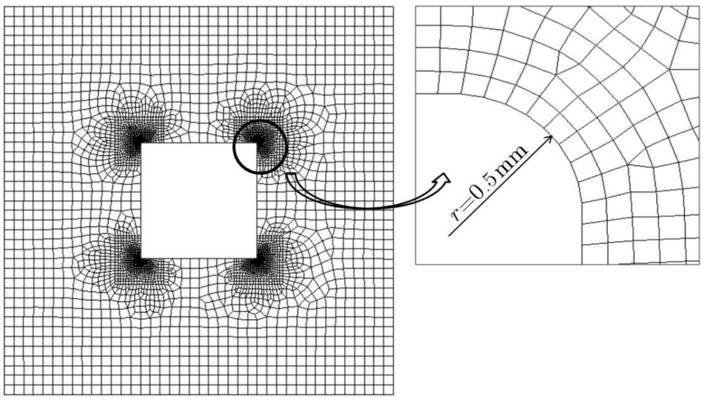

Fig. 3. Finite element model

4. Experimental approach

In this paper, the Digital Image Correlation (DIC) is used as an experimental method to determine the stress field and stress concentration factors on each radius. DIC represents a non-contact "state of the art" technique to measure and acquire full displacement, strain and stress fields of the structure, which is not possible using classical devices. Strain gauges cannot measure the full field and, however small, they cannot be placed on such a small corner radius ($r = 0.5\,\mathrm{mm}$).

The Digital Image Correlation compares the reference and deformed image by tracking their same physical points. The reference image is divided into "subsets" that represent a square matrix of pixels (Hild and Roux, 2006; Stoilov *et al.*, 2012). The digital images are recorded and processed using an image correlation algorithm which is based on the tracking of the grey value pattern in local subsets (Sutton, 2008). In order to determine a correspondence of each reference subset to the respective calculated subset in the deformed image, the correlation coefficient is defined (Lecompte *et al.*, 2006). The software calculates then the average gray scale intensity over the subset in the reference and deformed images and compares them.

The Aramis system, based on the DIC technique and used in this research, could be one of the first modern experimental methods that are able to "catch" stress results and full stress and strain fields in these small areas. The system consists of 3D cameras and a computer unit with the Aramis software. Two 3D cameras record the measurement and the computer unit (incorporated with the Aramis software) processes the results by recording full displacement fields and calculating strains and stresses (Ghafoori and Motovalli, 2011; Yu and Dehmer, 2010; Eriksen *et al.*, 2010).

Before even starting the measurement, calibration (Fig. 4) of the DIC installation needs to be performed. The calibration means taking photos of a series of images on an already defined calibration panel. This procedure defines 3D measuring volume and is extremely important for the measurement to be successful. If the parameters such as the camera angle, distance between cameras and measured object are in the prescribed range, the calibration is supposed to be performed correctly. Since the whole system is very sensitive, every movement of the cameras, sensors, lenses or modification of illumination in the laboratory can disrupt the measurement completely (Fazzini *et al.*, 2010). The measured surface has to be sprayed. The spray creates visible dots that make contrast between them and the surface. The system is monitoring the displacement of these dots. The level of contrast is directly linked to the accuracy of the process. A potential error can also be caused due to limited system resolution, statistical errors induced by calibration, subpixel effects resulting from limited camera resolutions, intrinsic uncertainties of the correlation algorithm, etc. (Schreier *et al.*, 2006). During the experiment performed, all error parameters (such as calibration deviation, defined angles and distance, illumination, etc.) are kept within the prescribed ranges to acquire more accurate results. Therefore, the obtained values are to be taken with the strain inaccuracy up to 0.01% and stress inacurracy up to 20 MPa for the used material (GOM mbH, 2009).

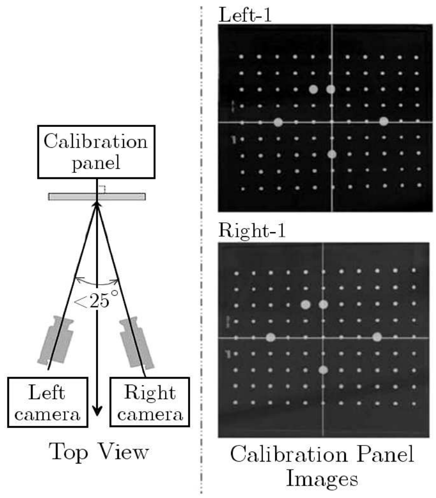

Fig. 4. Camera calibration

The Aramis system records dots, partitions dots into pixels and the pixels into smaller units called facets. Smaller facets capture localized effects better and therefore they are more convenient for a particular experiment of this research. By tracking the facet distance, position its their relative movement while changing the loads, the Aramis acquires the displacement, strain and stress fields. After performing the experiment, the DIC system is able to illustrate the results in form of von Mises stress, principal stresses or in each direction.

The experimental installation (Fig. 5) beside the DIC system, includes an acquiring system and an additional computer unit to obtain and process the information from the load cell and additional strain gauges. The strain gauges are placed in the middle of each side of the plate, symmetrically, with the purpose to prove that the load is subjected correctly (if not, the gauges would measure different strains). To ensure an equal load distribution along the edge of the plate, two stiff bars are welded on each side of the plate to transfer the force without deforming the plate itself. The load is subjected via a hydraulic compressor and cylinder, and increased gradually. The maximal subjected load has been kept around 20 kN in order to stay in the elastic area of the material behavior concerning the expected high SCF around the corners.

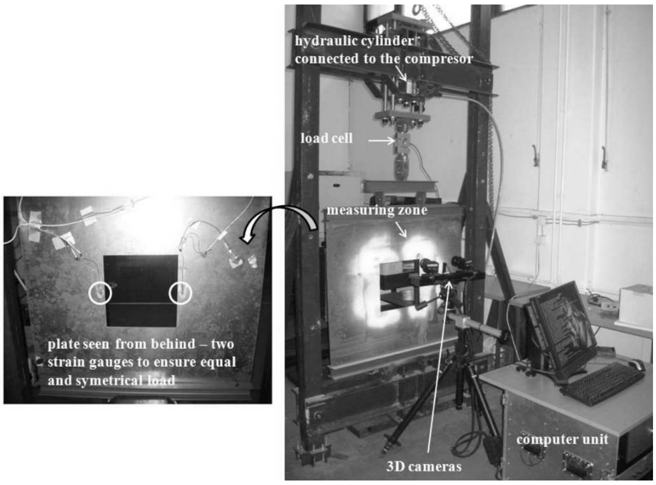

Fig. 5. Experimental installation

5. Results

For the analytical formula of the SCF (Motok, 1997) applied to the model investigated in this paper, the obtained results are presented in Table 2. The SCF is taken as the ratio of maximal principal stress in the point and the nominal tension load; a/r represents the ratio of the overall dimension of the opening and corner radius.

Table 2. SCF obtained analytically

a [mm]	r [mm]	a/r	SCF
300	0.5	600	16.7
300	1.0	300	12.7
300	2.0	150	9.8
300	3.0	100	8.3

In the numerical analysis, the load subjected to the model in FEM calculation is 20 kN, and the principal stress field for each radius is presented in the Fig. 6.

For the experimental procedure, the measurement had to be performed each time for each radius since the camera could record only one spot at one moment. The results of the experiment are illustrated in Fig. 7.

The analytical formula, finite element analysis and digital image correlation method offered fine matching of the results (Table 3, Fig. 8). Generally, there are some differences for smaller radii of corner curvatures and a very good correspondence for larger ones. The tendency of the results in all methods is the same. The finite element analysis provided the full stress field of the concerning zone, despite difficulties in mesh generation due to large differences in the dimension between the critical zone and the rest of the model. The DIC technique gave the full field results and even the change in the gradient, which is a step forward having in mind the available classical measuring devices. Rarely seen (but expected), a high SCF (especially for 0.5 and 1.0 mm of the radius) is well caught by all three methods.

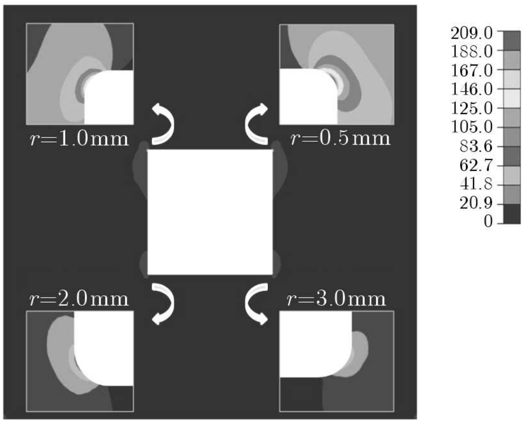

Fig. 6. Principal stress filed obtained by FEM, load applied – 20 kN

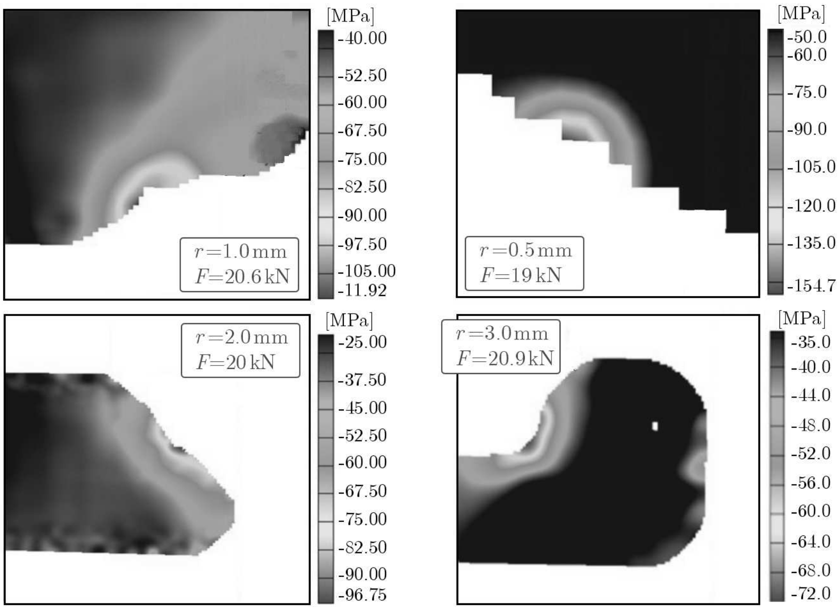

Fig. 7. Principal stress field obtained by the Aramis system

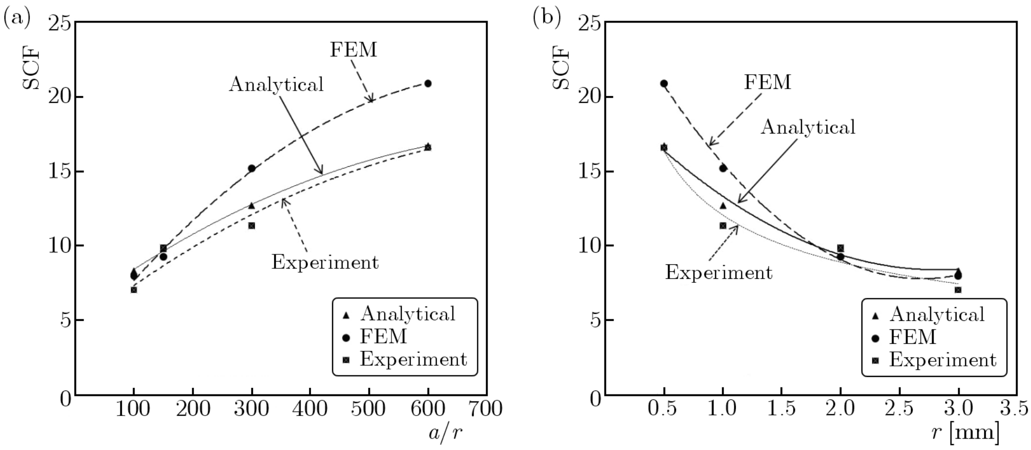

Fig. 8. SCF – comparison of the methods

Table 3. SCF – comparison of the methods

a [mm]	r [mm]	a/r	Analytical	FEM	Experiment
300	0.5	600	16.7	20.9	16.57
300	1.0	300	12.7	15.2	11.33
300	2.0	150	9.8	9.27	9.87
300	3.0	100	8.3	7.98	7.03

6. Conclusion

Corners of a rectangular plate openings are high stress concentration zones in daily structure application, especially if made with a significantly small radius of curvature. The paper presents and compares three possible methods for finding stress concentration factors (SCF) in such models. The chosen analytical method appears very easy to use, due to a simple formula, but can not provide the stress gradient field as the finite element analysis can. An analytical definition of the opening contour by means of conformal mapping remains a problem. As expected, the finite element analysis is able to provide the full stress field in the contour of the radius and to illustrate such a stress gradient. However, a very fine mesh density and adjusting is needed to obtain valid results, which increases computation time vastly. Until recently, there was no experimental method that could have been able to catch stress concentration of such small spots of radii of 0.5 or 1 mm. In such zones, the stress gradient changes within a millimeter distance. Strain gauges, inductive sensors and other classical devices are too large to be evenly placed on the spot. The Aramis system, used in this research, with the incorporated Digital Image Correlation technique, was capable to validate the numerical and analytical procedures, obtain the SCF and illustrate the stress and strain fields. All three methods produced very similar results, especially where larger corner radii of openings are placed. For those cases, both analytical and FEM approaches differ around 6% from the experimental results. For spots with higher SCFs, the numerical method gave a slightly greater divergence but still illustrated the stress gradient change in the zone very well.

The analytical formula showed almost no difference from the DIC results even in these areas. It can be stated that the DIC validated chosen analytical and numerical approaches as legitimate solutions for the problem. The DIC is still developing and is under research. Although used over the past few years, there are rare available data for the application of this experimental method to catch significantly high gradients. The technique is extremely sensitive and depends on the illumination, camera angle, contrast made by spraying, which all can influence the accuracy of the results (up to 20 MPa for this experiment, thus smaller values of the SCF for 2 or 3 mm radius become more sensitive) but definitely presents up-to-date solution to record and calculate the displacement, strain and stress filed of any measuring volume.

References

1. Batista M., 2011, On a stress concentration around the hole in an infinite plate subjected to uniform load at infinity, *International Journal of Mechanical Sciences*, **53**, 254-261

2. Chen H.C., 1993, Special finite element including stress concentration effects of a hole, *Journal of Finite element Analysis and Design*, **13**, 249-258

3. Eriksen R., Berggren C., Boyd S.W., Dulieu-Barton J.M., 2010, Toward high velocity deformation characterization of metals and composites using Digital Image Correlation, *ICEM 14 – 14th International Conference on Experimental Mechanics*, **6**, pp. 8

4. Fazzini M., Mistou S., Dalverny O., Robert L., 2010, Study of image characteristics on digital image correlation error assessment, *Optics and Lasers in Engineering*, **48**, 335-339

5. Ghafoori E., Motovalli M., 2011, Analytical calculation of stress intensity factor of cracked steel of I- beams with experimental analysis and 3D image correlation measurements, *Engineering Fracture Mechanics*, **78**, 3226-3242
6. GOM mbH, 2009, Aramis v6.1 User Manual, 2009, Germany
7. Guo S., Morishima R., Zhang X., Mills A., 2009, Cutout shape and reinforcement design for composite C section beams under shear load, *Composite Structures*, **88**, 179-187
8. Hild F., Roux S., 2006, Digital image correlation: from displacement measurement to identification of elastic properties – a review, *Strain*, **42**, 2, 69-80
9. Jones R., Wykes C., 1989, *Holographic and Speckle Interferometry*, Cambridge University Press, Cambridge
10. Kopecki T., 2010, Numerical and experimental analysis of post-critical deformation states in tensioned plate weakened by the crack, *Journal of Theoretical and Applied Mechanics*, **48**, 1, 45-70
11. Kopecki T., 2011, Numerical-experimental analysis of the post-buckling state of a multi-segment and multi-member thin walled structure subjected to torsion, *Journal of Theoretical and Applied Mechanics*, **49**, 1, 227-242
12. Kreis T., 2005, *Handbook of Holographic Interferometry*, Wiley-WCH
13. Laughalam A., Igusa T., Park C., Choi S., Kim K., 2011, Analysis of stress concentrations in plates with rectangular openings by a combined conformal mapping – finite element approach, *International Journal of Solids and Structures*, **48**, 1991-2004
14. Lecompte D., Smits A., Bossuyt S., Sol H., Vantomme J., van Hemelrijck D., Habraken A.M., 2006, Quality assessment of speckle patterns for digital image correlation, *Optics and Lasers in Engineering*, **44**, 11, 1132-1145
15. Madani K., Touzian S., Feaugas X., Cohenduoz X., Ratwani M., 2010, Experimental and numerical study of repair techniques for panels with geometrical discontinuities, *Computational Material Science*, **48**, 83-93
16. Maneski T., 2005, Structure behavior analysis and diagnostics, *FME Transactions*, **33**, 89-95
17. Maneski T., Milosevic-Mitic V., 2010, Numerical and experimental diagnostics of structural strength, *Structural Integrity and Life*, **10**, 3-10
18. Motok M., 1997, Locus of the maximum stress in the rounded corner zone of the plate opening, *Saopstenja, Faculty of Mechanical Engineering Belgrade*, **1**, 38-40
19. Motok M., 1997, Stress concentration on the contour of the plate opening of an arbitrary corner radius of curvature, *Marine Structures*, **1**, 1-13
20. Muskhelishvilli N.I., 1953, *Some Basic Problems of the Mathematical Theory of Elasticity*, Monograph, P. Noordhoff, Groningen
21. Post D., 1987, Moiré interfeometry, *Handbook of Experimental Mechanics*, Prentice Hall
22. Rezaeepazhand J., Jafari M., 2010, Stress concentration in metallic plates with special shaped cutouts, *International Journal of Mechanical Sciences*, **52**, 96-102
23. Savin G., 1961, *Stress Concentration Around the Holes*, Pergamon Press, Oxford
24. Schreier H.W., Braasch J.R., Sutton M.A., 2006, Systematic errors in digital image correlation caused by intensity imterpolation, *Optical Engineering*, **39**, 11, 2915-2921
25. Stoilov G., Kavardzhikov V., Pashkouleva D., 2012, A comparative study of random patterns for digital image correlation, *Journal of Theoretical and Applied Mechanics*, **42**, 2, 55-66
26. Sutton M., 2008, Digital image correlation for shape and deformation measurements, *Handbook of Experimental Solid Mechanics*, Springer, 565-600
27. Toubal L, Karama M., Lorain B., 2005, Stress concentration in a circular hole in a composite plate, *Composite Structures*, **68**, 31-36

28. Ukadgaonker V.G., Kakhandki V., 2005, Stress analysis for an orthotropic plate with an irregular shaped hole for different in-plate loading conditions – Part 1, *Composite Structures*, **70**, 255-274

29. Wu H.C., Mu B., 2003, On stress concentrations for isotropic/orthotropic plates and cylinders with a circular hole, *Composites – Part B*, **34**, 127-134

30. Yu J.H., Dehmer P., 2010, Dynamic impact deformation analysis using high speed cameras and Aramis photogrammetry software, Army Research Laboratory – Report, USA

Manuscript received September 19, 2012; accepted for print April 23, 2013